Combined Experimental and Theoretical Investigation of Polar Organic Adsorption/Desorption from Model Carbonaceous Surfaces: Acetone on Graphite

Seokjoon Kwon,[†,‡] Justin Russell,[‡,§] Xiongce Zhao,[||] Radisav D. Vidic,[†] J. Karl Johnson,[||] and Eric Borguet*[,‡,§]

Department of Civil and Environmental Engineering, Department of Chemical and Petroleum Engineering, Surface Science Center, and Department of Chemistry, University of Pittsburgh, Pittsburgh, Pennsylvania 15260

Received November 29, 2000. In Final Form: January 4, 2002

Adsorption on carbonaceous surfaces is important for applications ranging from atmospheric processes in the upper atmosphere to nanotechnology, yet little is known about adsorption of simple polar molecules on even the simplest carbonaceous surface, graphite. Optical differential reflectance (ODR) and temperature-programmed desorption (TPD) were combined to investigate the adsorption and desorption of a volatile polar organic compound (acetone) on the basal plane of a model graphite surface (highly oriented pyrolytic graphite) under ultrahigh vacuum conditions. The ODR change induced by adsorption/desorption was shown to correlate with relative coverage as determined by TPD experiments. TPD spectra revealed the existence of monolayer, bilayer, and multilayer adsorption states. Adsorption was found to follow a Volmer−Weber rather than a layer-by-layer growth mode. Molecular simulation of acetone on planar graphite was used to compute the geometry and coverage of acetone in the first, second, and third layers. Acetone molecules at submonolayer coverages tend to lie approximately parallel to the graphite surface. The acetone dipoles are predicted to align to produce favorable dipole−dipole interactions in the adsorbed phase. The second and third layers show considerably more disorder than the monolayer. The bilayer begins to form when the total coverage is about 4.5×10^{-6} mol/m^2. At this coverage, the monolayer is about 75% full. The third layer begins at a coverage of about 7.6×10^{-6} mol/m^2 at which point the monolayer is over 90% complete. Thus, the simulations support the experimental observation of Volmer−Weber growth.

1. Introduction

The adsorption of airborne pollutants (acids, organics, and metal vapor) on carbonaceous surfaces, such as activated carbon and elemental carbon (soot), has attracted much experimental and theoretical interest in the past decades.[1,2] The adsorption of organic molecules on carbonaceous surfaces is also of importance to the lubrication and protection of surfaces of magnetic data storage media.[3] Recently, consideration of adsorption on carbon surfaces has been extended to new carbonaceous materials, such as carbon nanotubes.[4] However, there is still a lack of fundamental understanding of the surface physics and chemistry of carbonaceous surfaces including simple processes such as adsorption and desorption.

Optical techniques have been widely shown to be convenient, in situ, and real-time methods to investigate surface processes.[5] There are a number of merits to optical techniques. Compared with conventional surface probes, such as ion and electron spectroscopy, optical techniques are useful over a wide range of ambient conditions.[6−8] ODR (optical differential reflectance) is a simplified version of ellipsometry that monitors the change of surface reflectivity when the surface is modified by adsorption and/or desorption.[9,10] It is known that adsorption on metal surfaces changes the optical reflectance[11] in the IR and visible region for many chemisorbed systems, such as H on W(100),[12] CO on Pt(111),[13] and NO on Cu(111).[14] Ellipsometry has been applied to investigate physisorption on surfaces, resulting in estimation of coverage from optically determined film thickness.[7,15] ODR has been used quantitatively to investigate adsorption, desorption and diffusion kinetics of chemisorbed species, on metal surfaces, in ultrahigh vacuum (UHV).[8,16,17] ODR enables adsorbate coverage measurements during adsorption/desorption of physisorbed species on a metal surface.[6] In short, ODR is a simple, versatile surface sensitive probe.

This study reports the adsorption and desorption of a model adsorbent representative of a volatile polar organic

* To whom correspondence should be addressed.
[†] Department of Civil and Environmental Engineering.
[||] Department of Chemical and Petroleum Engineering.
[‡] Surface Science Center.
[§] Department of Chemistry.

(1) Ammann, M.; Kalbarer, M.; Jost, D. T.; Tobler, L.; Rossler, E.; Piguet, D.; Gaggeler, H. W.; Baltensperger, U. *Nature* **1998**, *395*, 157−160.
(2) Korpiel, J. A.; Vidic, R. *Environ. Sci. Technol.* **1997**, *31*, 2319−2325.
(3) Gellman, A. J. *Curr. Opin. Colloid Interface Sci.* **1998**, *3*, 368−372.
(4) Kuznetsova, A.; Mawhinney, D. B.; Naumenko, V.; Yates, J. T., Jr.; Lui, J.; Smalley, R. E. *Chem. Phys. Lett.* **2000**, *321*, 292−296.
(5) Halevi, P. E. *Photonic Probes of Surfaces*; Elsevier: New York, 1995; Vol. 2.
(6) Wong, A.; Zhu, X. Z. *Appl. Phys. A* **1996**, *63*, 1−8.
(7) Volkmann, U. G.; Mannebach, H.; Knorr, K. *Langmuir* **1998**, *14*, 4904−4907.
(8) Jin, X. F.; Mao, M. Y.; Ko, S.; Shen, Y. R. *Phys. Rev. B* **1996**, *54*, 7701−7704.
(9) Deleted by author on revision.
(10) Deleted by author on revision.
(11) Hsu, C. L.; MacCullen, E. F.; Tobin, R. G. *Chem. Phys. Lett.* **2000**, *316*, 336−442.
(12) Reutt, J. E.; Chabal, Y. J.; Christman, S. B. *Phys. Rev. B* **1988**, *38*, 3112−3132.
(13) Kuhl, D. E.; Lin, K. C.; Chung, C.; Luo, J. S.; Wang, H.; Tobin, R. G. *Chem. Phys.* **1996**, *205*, 1−10.
(14) Dumas, P.; Suhren, M.; Chabal, Y. J.; Hirschmugl, C. J.; Williams, G. P. *Surf. Sci.* **1997**, *371*, 200−212.
(15) Steiger, R. F.; Muller, R. H.; Somorjai, G. A.; Moraito, J. M. *Surf. Sci.* **1969**, *16*, 234−250.
(16) Dvorak, J.; Dai, H. L. *J. Chem. Phys.* **2000**, *112*, 923−934.
(17) Xiao, X.; Xie, Y.; Shen, Y. R. *Surf. Sci.* **1992**, *271*, 295−298.

10.1021/la001666+ CCC: $22.00
Published on Web 03/01/2002

compound (acetone) on the basal plane of highly oriented pyrolytic graphite (HOPG). There is growing interest in the use of HOPG as a model for adsorption on carbonaceous surfaces.[18] ODR and temperature-programmed desorption (TPD) experiments were performed and showed that the strong correlation between ODR, determined in real time, and relative surface coverage, determined a posteriori by TPD, for metal systems could also be extended to carbonaceous surfaces. Thus, we established that ODR could be used quantitatively to determine coverage on carbonaceous surfaces. Many environmental phenomena involving carbonaceous surfaces occur under conditions where standard UHV surface science techniques, such as TPD, cannot be applied, for example, at atmospheric pressure. ODR, on the other hand, can be employed under atmospheric pressure conditions and may prove to be a useful tool under such conditions. In addition, it was shown experimentally, and confirmed by molecular simulations, that the growth of acetone on HOPG follows a Volmer−Weber mode, implying that acetone shows incomplete wetting on graphite.

2. Experimental Setup

A stainless steel UHV chamber, pumped by a turbomolecular pump backed by a mechanical pump, provided a base pressure of 8×10^{-10} Torr after bakeout. The adsorbent sample was HOPG (grade SPI-1, SPI Supplies). A Cu block, mounted on a stainless steel liquid nitrogen reservoir, held two electrically isolated Cu rods that serve as a sample support. The temperature was measured with a K-type thermocouple (chromel−alumel) spot-welded to one of the Ta plates that fix the sample to the Cu rods. The location of the thermocouple was a compromise as spot welding to HOPG is not possible. In our experiment, different thermocouple locations may shift the absolute TPD peak location but not the relative peak location. This leads to the uncertainty reported in the desorption energies. The sample can be heated to 1300 K by resistive heating and cooled to 87 K by liquid nitrogen. The sample was cleaved in air, using Scotch tape, immediately prior to installation. After the chamber bakeout, the sample was annealed at 1000 K overnight. This procedure removes possible contamination adsorbed from the background.[19,20]

The chamber was equipped with an ion gauge and a quadrupole mass spectrometer (QMS, Stanford Research, AccuQuad300) to measure total and partial pressures in the chamber. The QMS was fitted with a stainless steel shield to ensure collection of molecules from the sample only during thermal desorption experiments.[21] The shield aperture could be repeatedly positioned to within <1 mm of the sample for TPD experiments and retracted about 20 mm to allow sample rotation and dosing. The sample was typically held at 91 K during dosing. The constant temperature ramping rate, typically 2.5 K/s, was provided by a computer interfaced (LabView) power supply. Gas exposure was performed by backfilling the chamber. Acetone pressure and exposure were monitored via the QMS partial pressure reading at 43 amu. Exposures are reported in langmuirs (1 langmuir = 10^{-6} Torr s), determined by uncorrected ion gauge readings calibrated to the mass spectrometer reading at 43 amu. The UHV chamber was equipped with several viewports for laser light access to the sample. The light source for optical differential reflectance was a low-cost laser pointer (Marlin P. Johnson & Assoc. Inc., model no. 8689-LZ). The maximum output was 5 mW centered at 655 nm. The laser beam passed through a polarizer (Lambda Research Optics Inc., model no. ppb-2506u-248) and half wave plate (Lambda Research Optics Inc., model no. WP-10QC-M)) on a rotatable mount, which allowed the relative intensity of p- and s-polarized light incident on the sample to be adjusted. The angle of incidence of the beam at the sample was 65 ± 2°. After reflection from the sample, the beam was divided into p- and s- polarized light via a polarizing beam splitter (Coherent, model no. 44-4703). Each component was detected separately by two commercially available photodiodes (Thorlabs, model no. DET110).

Table 1. Parameters for the Acetone Model Used in the Simulations[a]

	CH_3	C	O
σ (Å)	3.88	3.75	2.96
ϵ/k (K)	85	52.84	105.68
q (e)	−0.032	+0.566	−0.502

[a] The Lennard-Jones parameters are the diameter σ and well depth ϵ/k, where k is the Boltzmann constant. The charges are placed at the center of each Lennard-Jones site.

For the ODR experiments, the sample is initially cleaned by heating to 600 K. The graphite is then cooled back to 91 K, and the intensities of reflected p- and s-polarized light are equalized by adjusting the half wave plate. Acetone is dosed while the ODR signal is monitored. After the desired dose of acetone is completed, the temperature is ramped for desorption.

The experimentally measured normalized ODR change, Δ, is defined by

$$\Delta = \left(\frac{I_p - I_s}{I_p + I_s}\right) \approx \frac{\Delta R_p}{2R_p} \quad (1)$$

where R is the total reflectivity of the clean surface and ΔR is the reflectivity change due to adsorption and desorption. $\Delta R/R$ is a complex function of the incident angle as well as the optical properties of the adsorbate and substrate.[22] I_p and I_s refer to the intensity of p- and s-polarized light reflected from the substrate surface, respectively. I_p and I_s are related to the reflectivity, $I_s = R_s I_{os}$, $I_p = R_p I_{op}$, where I_{os} and I_{op} are the intensity of light incident on the surface and R_s and R_p are the reflectivity of s- and p-polarized light, respectively. The p-polarized light is the "signal" and the s-polarized light is used as the "reference" due to the fact that adsorbate-induced reflectivity changes depend on polarization, with p-polarized light being far more sensitive than s-polarized light to the presence of adsorbates.[23]

3. Molecular Simulations

Computer simulations of acetone adsorbed on graphite were performed in order to study the structural character and growth mode of the adsorbed phase. Acetone was modeled with a nonpolarizable potential.[24] The model consists of four Lennard-Jones sites to account for the CH_3, C, and O groups, plus explicit charges centered on each of the Lennard-Jones sites to account for the polar interactions. The Lennard-Jones and charge parameters are given in Table 1. The molecule was held rigid with CH_3-C bond lengths of 1.572 Å, a C=O bond length of 1.223 Å, a $CH_3-C=O$ bond angle of 121.35°, and a CH_3-C-CH_3 bond angle of 117.30°. The reaction field correction was applied to account for the long-range electrostatic interactions. The cutoff for the Lennard-Jones interactions was taken to be about 15 Å. The acetone−graphite interaction was computed from the 10-4-3 potential developed by Steele[25] plus induction and quadrupole interactions to account for the charge sites on acetone interacting with the graphite surface.[26] The 10-4-3 parameters were computed from the Lorentz−Berthelot combining rules. Canonical ensemble (NVT) Monte Carlo simulations were performed to generate equilibrium configurations of adsorbed acetone at fixed coverage. The

(18) Dorko, M. J.; Bryden, T. R.; Garrett, S. J. *J. Phys. Chem. B* **2000**, *104*, 11695−11703.
(19) Blum, B.; Salvarezza, R.; Arvia, A. *J. Vac. Sci. Technol., B* **1999**, *17*, 2431−2438.
(20) Palmer, R. E.; Kenny, D. J. *Surf. Sci.* **2000**, *447*, 126−132.
(21) Schlichting, H.; Menzel, D. *Surf. Sci.* **1993**, *285*, 209−218.
(22) McIntyre, J. D. E.; Aspnes, D. E. *Surf. Sci.* **1971**, *24*, 417−434.
(23) Dvorak, J.; Borguet, E.; Dai, H. L. *Surf. Sci.* **1996**, *369*, L122−L130.
(24) Jedlovszky, P.; Pallinkas, G. *Mol. Phys.* **1995**, *84*, 217−233.
(25) Steele, W. A. *Surf. Sci.* **1973**, *36*, 317−352.
(26) Zhao, X.; Johnson, J. K. Manuscript in preparation.

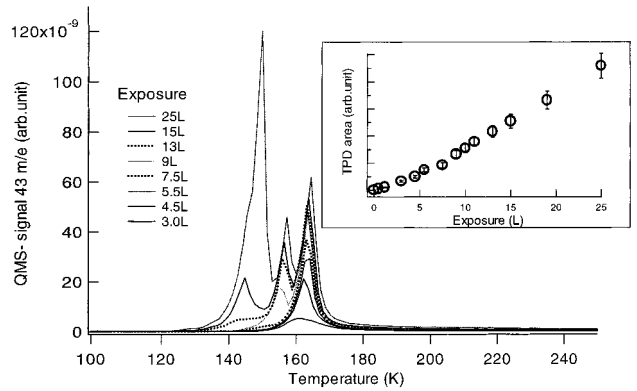

Figure 1. TPD spectra of acetone from graphite following adsorption at 91 K. The inset shows the integrated TPD data area vs exposure.

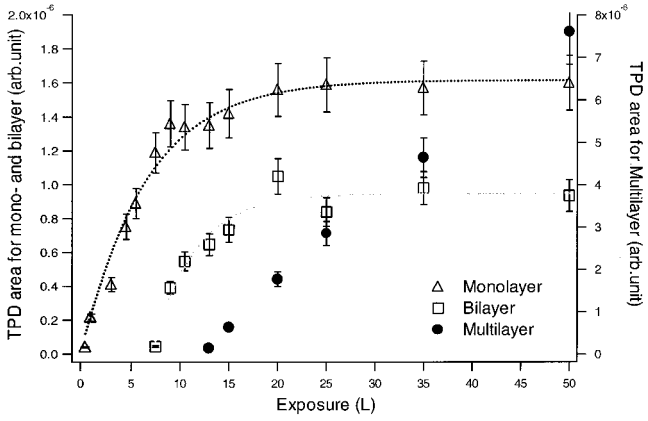

Figure 2. Integrated area of monolayer, bilayer, and multilayer TPD features. The dotted lines are fits assuming the adsorption follows Langmuir kinetics. The bilayer peak begins to grow after the first layer has reached 70% of its saturation coverage. The multilayer peak appears when the bilayer is at about 75% of its saturation coverage.

simulation cell consisted of one surface representing the basal plane of graphite with a repulsive (reflecting) wall fixed opposite the graphite plane. The distance between the graphite plane and the reflecting wall was 59 Å. Periodic boundary conditions were applied in the remaining two directions. One or more layers of acetone molecules were placed in close proximity to the graphite surface in order to generate the initial configurations. Different coverages were simulated by varying the number of layers of acetone in the box. The system was equilibrated for 2 million moves. Each move consisted of either a random displacement or a random reorientation of an acetone molecule. The maximum displacement and reorientation parameters were adjusted during equilibration to achieve approximately a 50% acceptance rate for each type of move. Data taking for an additional 2 million moves followed equilibration. A few very long *NVT* simulations were performed to check the long-time stability of the structures. These longer simulations consisted of up to 150 million moves.

Molecular simulations of acetone adsorption were also carried out in the grand canonical Monte Carlo (GCMC) ensemble wherein the chemical potential, volume, and temperature of the system are held fixed and the number of molecules adsorbed on the surface is changed through randomly inserting and deleting molecules in the simulation cell.[27] Because of the size and polarity of the acetone molecule, conventional GCMC simulations are extremely inefficient for inserting and deleting molecules. We have implemented orientationally biased GCMC[28] to improve the efficiency of the calculations. Each attempted insertion or deletion of a molecule utilized information from five random orientations. The GCMC simulations were carried out at 90 and 150 K. Simulations were equilibrated for 50 million moves, consisting of displacements, reorientations, insertions, and deletions, attempted with equal probability. Data were collected over an additional 50 million GCMC moves. The average number of acetone molecules in the simulation box varied between 110 and 280. The potential cutoff for the GCMC simulations was set to about 10 Å.

4. Results and Discussion

4.1. TPD. The results of TPD experiments are shown in Figure 1. The area under each curve is proportional to the surface coverage. Each peak in the TPD spectra corresponds to the temperature of maximum desorption rate. In the lowest exposure data, until 7.5 langmuir, only one peak is seen at about 165 K. For exposures >7.5 langmuir, two peaks are seen at about 155 and 165 K. For 15 langmuir exposure, three peaks can clearly be seen at around 145, 155, and 165 K. The three characteristic peaks are still present at higher exposure with the lowest temperature peak growing the most. The integrated TPD area versus exposure is also shown in the inset in Figure 1.

Each TPD feature is associated with molecules desorbing from different surface layers, in agreement with a literature report for acetone desorption from a graphitic layer on Pt(111).[29] The highest temperature peak (~165 K) represents desorption from the monolayer.[16,29] The second TPD peak (~155 K) is associated with desorption from the bilayer.[29] The lowest temperature TPD peak (at about 145 K) represents desorption from the multilayer.[16,29] Figure 2 illustrates the growth of the TPD area of the monolayer and bilayer peaks calculated by deconvolution. The dotted lines are the fitting curves assuming that adsorption follows Langmuir kinetics. The bilayer peak begins to grow after the first layer has reached about two-thirds of its saturation coverage. The similarity of the slopes of the Langmuir fits for both monolayer and bilayer indicates that the sticking probabilities of acetone on the HOPG surface and on the monolayer are similar. The appearance of the multilayer peak in the TPD spectra (Figures 1 and 2), at about 13 langmuir, indicates the point at which molecules begin to adsorb on the bilayer. Again, the multilayer peak appears before the bilayer feature has saturated. The data in Figure 2 indicate that the monolayer is about 90% complete and the bilayer is about 75% complete when the multilayer appears. The data suggest that the adsorbates grow according to a Volmer−Weber mechanism rather than a layer-by-layer mode.[30] Figure 3 illustrates the proposed adsorption sequence. At low exposure, acetone molecules adsorb directly on the surface, in a monolayer state. The appearance of a second peak before the monolayer completely saturates suggests that in addition to molecules binding on the HOPG surface, acetone molecules begin to bind to the monolayer, thereby creating a bilayer. As the bilayer feature grows, the monolayer feature continues to increase,

(27) Allen, M. P.; Tildesley, D. J. *Computer Simulation of Liquids*; Clarendon Press: Oxford, 1987.
(28) Smit B. *Mol. Phys.* **1995**, *85*, 153−172.
(29) Dinger, A.; Lutterloh, C.; Biener, J.; Kuppers, J. *Surf. Sci.* **1999**, *437*, 116−124.
(30) Zangwill, A. *Physics at Surfaces*; Cambridge University Press: New York, 1988.

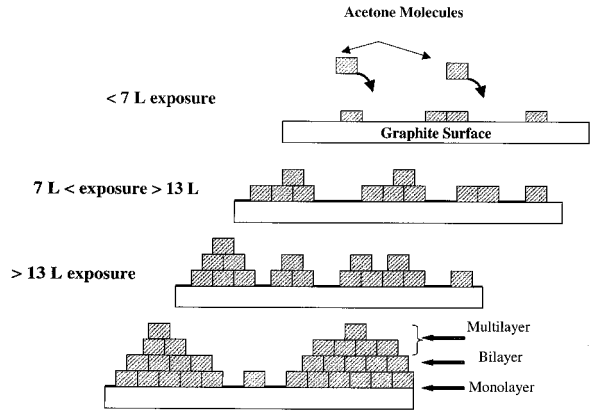

Figure 3. Schematic drawing of the proposed topological growth mode (Volmer−Weber) of acetone on graphite at 91 K. The bilayer appears before the monolayer state is completely saturated. As the bilayer feature grows, the monolayer feature continues to increase, though more slowly. The multilayer also appears before monolayer or bilayer saturation has been achieved.

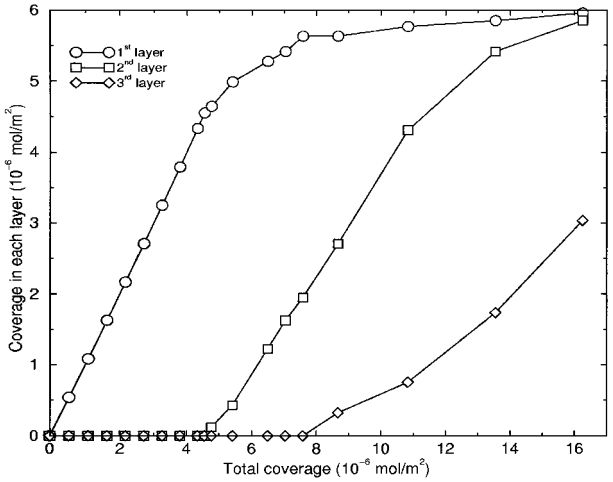

Figure 4. The coverage of acetone adsorbed in each layer, determined from *NVT* simulations at 91 K, as a function of total loading. Note that the second layer begins to form well before the first layer is complete. Likewise, the third layer appears before the first or second layer is complete.

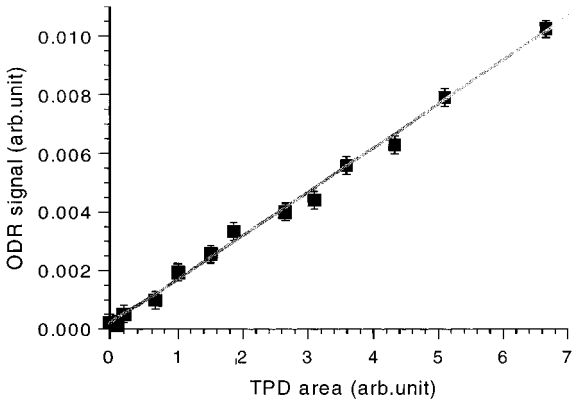

Figure 5. Correlation between ODR and TPD experiments for acetone adsorption on graphite. The solid line is a straight-line fit of the experimental data ($R^2 = 0.995$). The correlation of the ODR signal and TPD area suggests that ODR indeed measures the surface coverage change induced by adsorption.

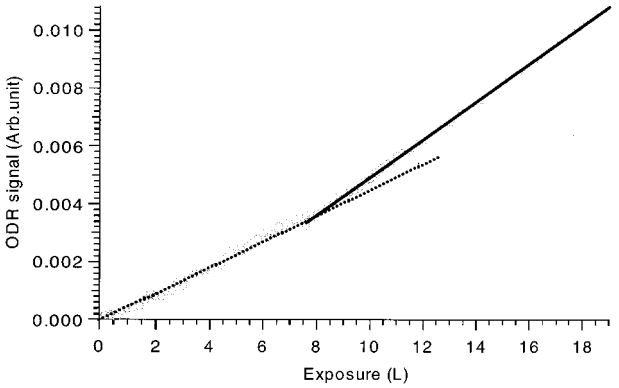

Figure 6. The ODR signal as a function of acetone exposure at 91 K. The ODR signal increases linearly until about 7.5 langmuir exposure (dashed line) at which point the bilayer has begun to grow and the slope of the increase (solid line) becomes steeper at higher exposure.

though more slowly, indicating that there are still bare HOPG sites to be filled. These findings are supported by the results of the molecular simulations. Figure 4 is a plot of the adsorption coverage, determined by the *NVT* simulations, in each layer as a function of the total coverage. The second layer begins to grow at a total coverage of about 4.5×10^{-6} mol/m^2, at which point the monolayer is about 75% full. This is in reasonable quantitative agreement with the estimate from the TPD spectra showing bilayer growth at about 70% of monolayer saturation. The simulation data in Figure 4 confirm that the third layer begins to grow before the second layer is filled, which also agrees with the TPD data. To address the reproducibility of our results, TPD experiments using a different high-quality HOPG sample (Grade ZYA, Advanced Ceramics) were performed. These show essentially the same results; three-peak TPD spectra and Volmer−Weber growth of acetone.

Additional simulations in the *NVT* ensemble were run for very long times at a coverage that would correspond to monolayer completion. The simulations indicate that the Volmer−Weber growth model is apparently a kinetic phenomenon rather than the equilibrium configuration. The simulations show that molecules from the second layer slowly relax to the first layer over the course of the run. However, even after 150 million moves not all molecules in the second layer were able to diffuse to the first layer. The *NVT* simulations are more closely related to the experimental situation because molecules strike the surface very rapidly and then slowly relax in both cases. Simulations in the GCMC ensemble put molecules on the surface one-by-one with relaxation of the adsorbate molecule taking place as new molecules are added to the system. Our GCMC simulations show that when acetone is added slowly to the surface, a complete monolayer is formed before adsorption in the second layer starts. Thus, the equilibrium situation is for layer-by-layer growth rather than Volmer−Weber. However, the *NVT* simulations show that Volmer−Weber growth is indicated when adsorbate molecules are added rapidly to the system.

Monolayer, bilayer, and multilayer TPD peaks are observed for acetone on a graphitic layer on Pt(111)[29] and acetone on Ag(111).[31] The "bilayer" peak saturates at a lower coverage than the "monolayer" peak on Ag(111).[31] While Dinger et al. attribute the second peak to the formation of a bilayer,[29] White et al. do not attribute the second TPD peak to bilayer formation. Rather, they suggest that adsorbate−substrate interaction competes with interadsorbate interaction inducing coverage de-

(31) Sparks, S. C.; Szabo, A.; Szulczewski, G. J.; Junker, K.; White, J. M. *J. Phys. Chem. B* **1997**, *101*, 8315−8323.

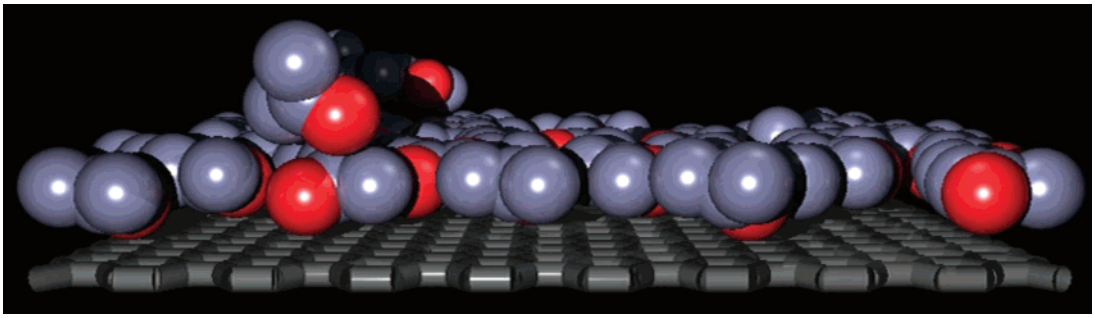

Figure 7. A simulation snapshot of acetone adsorbed on graphite at a coverage of 4.8×10^{-6} mol/m^2. The red (light) spheres are the oxygen atoms, the gray (dark) spheres are the methyl and carbonyl groups. Note that molecules in the first layer lie almost parallel to the surface.

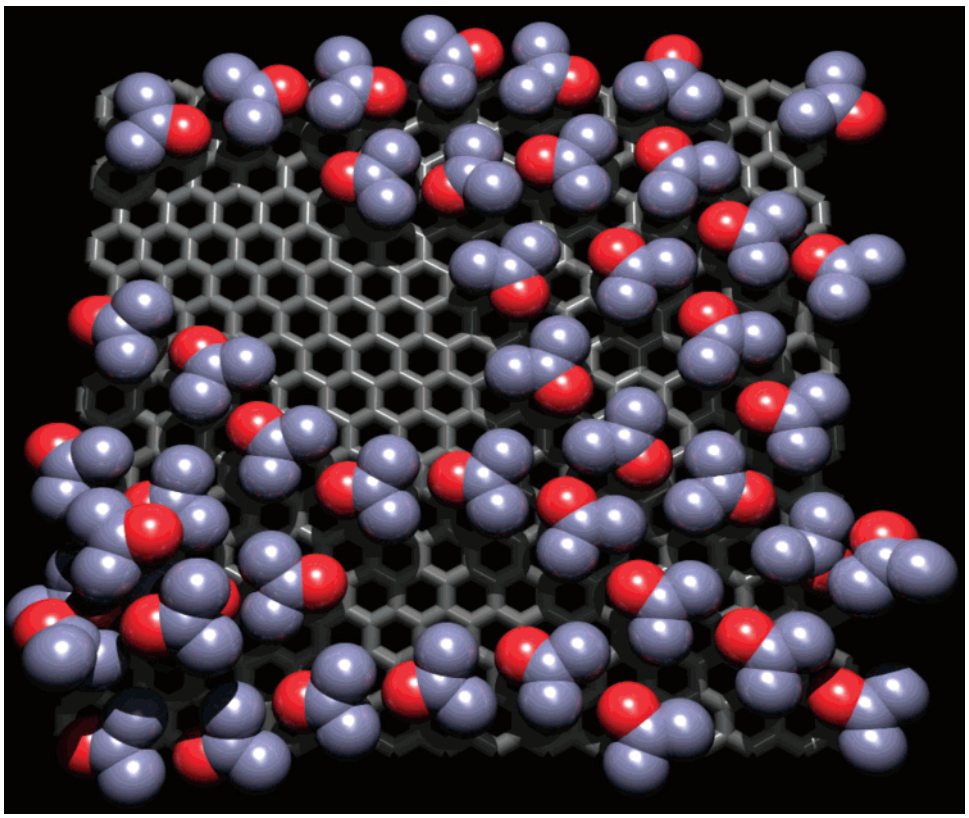

Figure 8. A top-down view of the simulation snapshot shown in Figure 7. Note that the dipoles tend to order into local domains so that the dipole−dipole interaction is favorable. The graphite surface is not completely covered at this coverage, revealing an incomplete first layer. Molecules adsorbed in the second layer are apparent in the lower lefthand corner for example.

pendent structures, resulting in the monolayer and bilayer peaks. Their isotope mixing experiments show that intermixing occurs between the layers at the adsorption temperature or upon heating. This makes it difficult to assign the integrated area in each peak with the coverage of each layer. The lower coverage of the bilayer could result from some bilayer molecules converting to monolayer species as the monolayer sites are made available due to desorption of monolayer species. The monolayer sites are energetically more favorable than bilayer sites by several kJ/mol as evidenced by their higher desorption temperatures. The monolayer and bilayer TPD peaks overlap, and some monolayer species have desorbed prior to depletion of the bilayer, consistent with the hypothesis of layer exchange. The hypothesis of layer exchange is indirectly supported by the simulations, which show that the bilayer saturation coverage is the same as the monolayer saturation coverage (Figure 4). The absolute coverage at which the bilayer and multilayer features appear can be estimated, in principle, from optical difference reflectance.

The thermal desorption spectra of the acetone multilayer state are described by a zero-order rate law, because of the observed invariance of the leading edge of the TPD spectra to changes in the initial coverage of the adsorbate.[32] The activation energy for desorption of the acetone multilayer from graphite was determined to be 31 ± 2 kJ/mol. This is in agreement with the sublimation energy of acetone, 31 kJ/mol.[33,34] The excellent agreement between the multilayer desorption energy determined in this study and the bulk enthalpy of sublimation suggests that sample temperature readings are quite accurate (±2 K) and that the adsorbate is pure. Our results can be compared to the

(32) King, D. A.; Madey, T. E.; Yates, J. T., Jr. *J. Chem. Phys.* **1971**, *55*, 3247−3253.
(33) *CRC Handbook of Chemistry and Physics*, 78th ed.; Lide, D. R., Ed.; CRC Press: London, 1997.
(34) *Lange's Handbook of Chemistry*, 5th ed.; Dean, J. A., Ed.; McGraw-Hill: New York, 1999.

TPD spectra of other polar organic adsorbates (alcohols and ethers) on HOPG that showed first-order monolayer and zero-order multilayer desorption peaks.[35,36]

4.2. Optical Differential Reflectance (ODR). 4.2.1. Adsorption Experiments. ODR experiments were performed by continuous exposure at 1.2×10^{-7} Torr of acetone pressure with the HOPG sample at 91 K. To validate ODR as a quantitative technique, the optical reflectivity change should correlate with coverage as determined from TPD, for example. Control experiments indicate that p-polarized light is much more sensitive to adsorption than s-polarized light. This confirms the use of p-polarized light as a signal and s-polarized light as a reference. Figure 5, a plot of the ODR signal as a function of TPD area, shows a linear correlation ($R^2 = 0.995$) between these techniques, suggesting that ODR indeed measures the surface coverage change induced by adsorption. The correlation also indicates that the TPD spectra are free from contributions due to desorption from other surfaces in the chamber. Note that the ODR only probes a small area (<1 mm^2) in the center of the HOPG sample. Spurious signals that might arise from outgassing of the sample mount and that might be detected with an inadequately shielded QMS do not contribute to ODR.

The near linearity of the ODR with exposure, Figure 6, suggests that overall acetone adsorption on graphite does not follow simple Langmuir adsorption kinetics. However, the individual monolayer and bilayer states do follow Langmuir adsorption kinetics (Figure 2). As can be seen in Figure 6, the ODR signal increases linearly until about 7 langmuir exposure (dashed line) at which point the bilayer has begun to grow and the slope of the ODR (solid line) becomes steeper. Similar behavior is observed for the integrated TPD area versus exposure (inset to Figure 1). While the mono- and bilayer appear to follow Langmuir kinetics (Figure 2), the multilayer does not. This is most likely the origin of the apparent increased sticking probability for the multilayer and the increase in uptake at higher exposures.

4.2.2. Quantitative ODR for a Physisorbed System: Three-Layer Model. The reflectivity change induced by adsorption/desorption of a physisorbed species can be described by a three-layer model.[22] The acetone overlayer "thickness" for 7 langmuir exposure, the point at which the bilayer begins to grow, can be estimated using this model assuming that graphite, in a first approximation, is an optically isotropic substrate.[22] Using as the optical dielectric constants 1.846 for acetone[33] and 5.04 + i8.4 for the substrate (graphite),[37] the ODR signal (0.35%) in Figure 6 corresponds to a thickness of 5 ± 2 Å. The overlayer thickness at which the multilayer begins to grow is calculated from the ODR signal (0.65%) for 13 langmuir exposure to be 10 ± 3 Å. Errors in the film thickness estimation originate from the ODR noise and the accuracy of the incident angle measurement. The ODR thickness compares favorably to the thickness of a single layer estimated from the simulations that indicate that the locus of the first layer lies at about 3.5 Å above the graphite, that of the second layer is located at 7 Å above the surface, and the third is at 10.5 Å. We define the surface as the location of the carbon atom centers of mass in the first graphitic layer.

The molecular simulations show that the average angle between the dipole moment of the acetone molecules in the first layer and the graphite surface normal is about 80°. Likewise, the angle between the molecular and graphite planes for molecules in the first layer is about 10°. The molecules are pointed slightly down, with the oxygen atoms pointing toward the graphite plane. This orientation can be observed in the snapshot from the simulations shown in Figure 7. This is a side view of molecules that are primarily adsorbed in the first layer. A top-down view of the same snapshot is shown in Figure 8. It can be seen from this figure that the dipoles tend to align into local domains such that the dipole−dipole energy is minimized.

5. Conclusion

The adsorption/desorption of a model adsorbent representative of a volatile organic compound (acetone) on the basal plane of a model carbonaceous surface (graphite) has been investigated under ultrahigh vacuum conditions. ODR provides a sensitive, noninvasive, in situ, and direct probe of surface coverage with real-time resolution. TPD experiments show that acetone adsorbs in distinct monolayer, bilayer, and multilayer states on graphite at 91 K, suggesting Volmer−Weber growth rather than layer-by-layer growth. The Volmer−Weber growth is also observed in molecular simulations, showing that the second layer begins to form when the first layer is about 75% full, and the third layer starts before the completion of the first or second layers. Molecular simulations show that acetone adsorbs nearly parallel to the graphite surface in the first layer, but some molecules begin to orient perpendicular to the surface as the second layer forms. It is concluded that ODR is a suitable analytical technique to investigate adsorption/desorption or any other phenomenon resulting in a change in coverage of weakly bound species on carbonaceous surfaces over a wide pressure range and in real time.

Acknowledgment. The authors acknowledge useful discussions with Professor J. T. Yates, Jr., and his group. This work is supported by the U.S. Department of Energy under Grant No. DE-FG26-98FT40119. Justin Russell acknowledges the support of the NSF-REU program (PHY99-87904) at the University of Pittsburgh. Calculations were performed at the Center for Molecular and Materials Simulation at the University of Pittsburgh.

LA001666+

(35) Shukla, N.; Gui, J.; Gellman, A. J. *Langmuir* **2001**, *17*, 2395−2401.
(36) Lei, R. Z.; Gellman, A. J. *Langmuir* **2000**, *16*, 6628−6635.
(37) *Handbook of Optical Constants of Solids II*; Palik, D., Ed.; Academic Press: New York, 449.